

Two dimensional expansion effects on angular distribution of 13.5 nm in-band extreme ultraviolet emission from laser-produced Sn plasma

K. L. Sequoia,^{a)} Y. Tao, S. Yuspeh, R. Burdt, and M. S. Tillack
*Department of Mechanical and Aerospace Engineering and the Center for Energy Research,
 University of California, San Diego, 9500 Gilman Drive, La Jolla, California 92093-0438, USA*

(Received 4 March 2008; accepted 13 May 2008; published online 3 June 2008)

The angular distribution of extreme ultraviolet emission at 13.5 nm within 2% bandwidth was characterized for laser irradiated, planar, Sn targets at prototypic conditions for a lithography system. We have found that two dimensional plasma expansion plays a key role in the distribution of in-band 13.5 nm emission under these conditions. The angular distribution was found to have two peaks at 45° and 15°. This complex angular distribution arises from the shape of both the emitting plasma and the surrounding absorbing plasma. This research reveals that the detailed angular distribution can be important to the deduction of conversion efficiency. © 2008 American Institute of Physics. [DOI: 10.1063/1.2938717]

Extreme ultraviolet lithography (EUVL) is the leading candidate for the next generation of lithography systems, which will push node sizes to 32 nm or below.¹ Development of an efficient, powerful, long-lifetime, and affordable extreme ultraviolet (EUV) source is one of the main challenges in the development of an EUVL system. Laser-produced Sn plasma is one of the most promising EUVL sources. Accurate measurement of the conversion efficiency (CE) from laser energy to in-band EUV energy is a critical issue in the optimization of an EUV source. In a typical experiment, the in-band EUV emission is measured at a fixed angle with respect to the target normal and an assumption is made about how the emission will vary with angle.²⁻⁵ Based on the single measurement, the emission is calculated over a 2π solid angle to estimate the total EUV energy that can be collected. To apply this method effectively, an accurate description of the angular distribution is important.

The density profile plays a key role in the generation and transport of 13.5 nm EUV emission in laser-produced Sn plasmas due to its high opacity. Moreover, the plasma density strongly depends on the particular experimental conditions, such as laser intensity, pulse duration, focal spot size, and target geometry. Detailed angular distribution measurements may be necessary for each particular experimental condition.

A detailed description of the present experimental arrangement can be found elsewhere.⁶ A high-purity Sn slab was positioned at the center of a vacuum chamber and heated with a 1.064 μm laser. The $1/e^2$ laser spot size was 150 μm and the pulse energy and duration were 250 mJ and 8 ns, respectively, in order to be relevant to a commercial device.⁷ A fresh target surface was used for each shot. A probe beam passes through the plasma parallel to the target surface, 90° with respect to the target normal and heating laser. Phase shift induced by the plasma density profile is recorded by a Nomarski interferometer.⁶ In-band 13.5 nm EUV light was measured with an absolutely calibrated EUV energy monitor (E-Mon) positioned 45° from the target normal and a transmission grating spectrometer (TGS) positioned 90° from the E-Mon.

Angular measurements were made by mounting the target on aluminum wedges with angles of 15°, 30°, or 45°, making the angles to the E-Mon 30°, 15°, or 0°, respectively. Flipping the wedges gives 60°, 75°, and 90°. No wedge is used for the 45° measurements. The TGS data are collected simultaneously for the complementary angles. The pump beam is normal to the target surface except for the two extreme angles, where the beam propagates at 5° to the target normal. This small angle does not significantly change the intensity on target. In each case, except the 45° measurements, two broadband mirrors are used to align the pump beam with the target normal. Laser energy losses due to the mirrors are not significant enough to affect the CE. The position of the target surface in the chamber and the distance to the focusing lens are fixed for all angles. Five data points were acquired at each angle. To rule out alignment errors, the alignment and measurement process was repeated to get a second fully independent set of data at each angle.

Figure 1 shows the angular dependence of the in-band EUV emission. Blue triangles are the data measured by the E-Mon and blue dashed line is a smooth fit of the data. Red dots represent the data from the TGS, and the red line represents a smoothed fit. The spectrometer data are obtained by integrating the in-band portion of the spectra and normaliz-

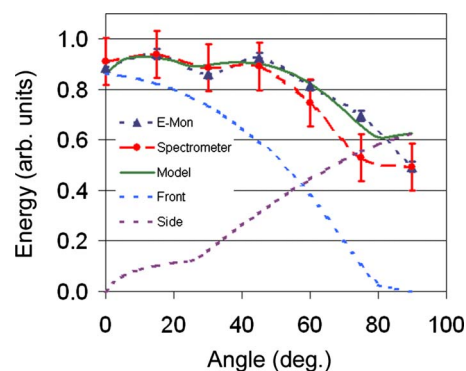


FIG. 1. (Color online) EUV emission at various angles measured with the E-Mon (blue dashed line), TGS for comparison (red dashed line), and modeled values (green line) with front and side surface components (light blue and purple dashed lines). TGS and calculated values are scaled to match the E-Mon measurements.

^{a)}Electronic mail: sequoia@fusion.ucsd.edu.

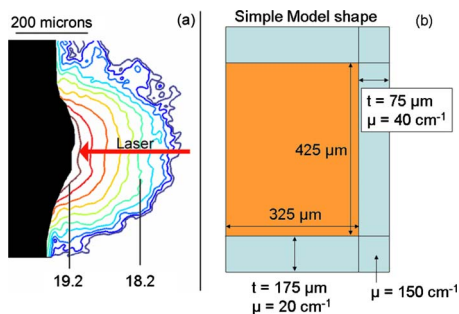


FIG. 2. (Color online) (a) Log_{10} of the plasma density at the peak of the laser pulse. The arrow indicates the pump laser direction. (b) Modeled plasma shape with the emitting plasma (orange) and the surrounding plasma (blue).

ing to the E-Mon measurements. It should be noted that the spectrometer is not a calibrated instrument, and is much more sensitive to alignment than the E-Mon. The disagreement at larger angles is likely due to a small misalignment at these angles or slight asymmetry in the plasma. The spectrometer data are only mentioned here as a confirmation of the dip found in the E-Mon data. The most notable features of the data are the dips at 0° and 30° . These dips were not measured in previous studies possibly because of the limited number of measurement angles in those studies, but more likely because of two dimensional (2D) plasma expansion.^{8–12} The earlier works used a relatively large laser spot size, around $500 \mu\text{m}$ compared to $150 \mu\text{m}$ used here, or the laser was not at normal incidence on the target, which would change the angular distribution. The smaller spot size leads to similar scales for the lateral and longitudinal plasma expansions. This allows the side of the plasma to make a significant contribution to the overall emission. A small focal spot size is needed in a practical EUVL source system to match the limited size of the mass-limited droplet target.

Figure 2 shows the plasma density calculated from the interferogram observed at the peak of the 8 ns Gaussian laser pulse with the Nomarski interferometer, the mathematic methods used to deduce the plasma density profile from an interferogram have been described in previous works.^{13,14} The in-band EUV is mainly produced where the plasma density is around 10^{19}cm^{-3} .¹⁵ This region absorbs the in-band light, so photons produced in the inner most regions do not reach the detector. The surrounding plasma acts to absorb the in-band light.

The EUV spectra for various angles can be seen in Fig. 3. It is worth noting that more emission is seen at wavelengths longer than 13.5 nm as the angle moves toward 0° , which reveals a broad distribution of Sn ionization states along the laser axis. In addition, there is a dip located in the in-band region of the spectra at these smaller angles caused by reabsorption from the EUV plasma itself.¹⁴ For large angles, the spectra are narrower and the out-of-band emission can be explained by blackbody radiation, indicating a more uniform ionization along the sides.

In order to clarify the effect of 2D plasma expansion on the angular distribution of the in-band EUV emission, a simple model based on 2D plasma expansion is employed to qualitatively explain our data. The emission from a surface can be described by $f(\theta) = \alpha + \beta \cos^2 \theta$, and the absorption by $\exp[-\mu t / \cos(\theta)]$, where μ is the absorption coefficient, t is the thickness of the absorption region, and θ is the angle

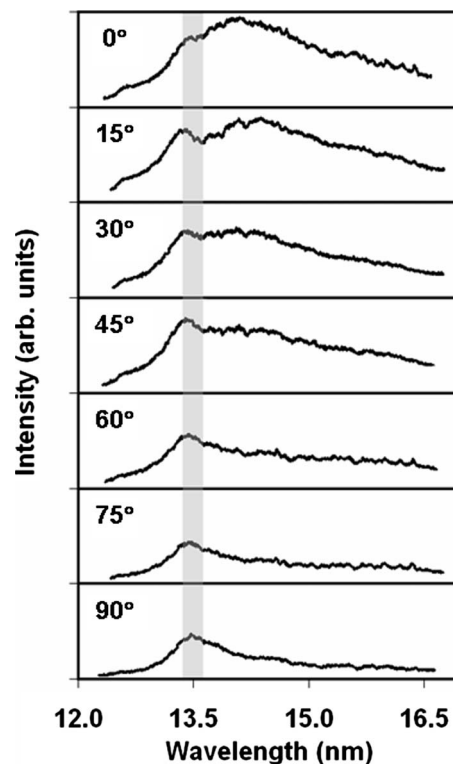


FIG. 3. Typical soft x-ray spectra measured at each angle with the 2% in-band spectral range shaded.

between the detector and the target normal.⁹ The value of γ has been empirically determined to be 0.5 for a $1.064 \mu\text{m}$ laser.⁹ In Fig. 2(b), a simplified sketch of the plasma used for the calculation is shown. The plasma is modeled as a rectangular emitting region surrounded by three rectangular absorbing regions. The detectable emission from each surface is calculated independently using the above method. The total signal is just the sum of the front surface and one side surface. Only one side surface is counted since the high-density plasma would absorb the emission from the back side. The calculated angular distribution can be seen in Fig. 1. Contributions from each surface are also shown. This calculation assumes that the emitting and absorbing regions emit and absorb uniformly. It can be seen that the dip near 25° is caused by the in-band emission from the side of the plasma being absorbed in the more optically thick corner region.

We have shown that the EUV angular distribution is affected by 2D plasma expansion for small laser spot sizes. In cases where the spot size is larger than a few hundred microns, the expansion is almost one dimensional so the sides of the plasma do not make a significant contribution to the emission. When the spot size is smaller than a few hundred microns, the emitting region has similar scales along the lateral and longitudinal directions making the overall emission the sum of the emission from the front and one side of the plasma. The detected light is just the overall emission with the proper attenuation due to the plasma between the emitting region and the detector, and the absorption is less in the longitudinal direction. In a practical EUVL source system, a small size mass-limited target, like a droplet with diameter from several 10 to a couple of $100 \mu\text{m}$, is necessary to mitigate debris and save the fuel. In order to get high CE, small focal spot size is required to match the target size. So the

detailed angular distribution of EUV emission arising from two dimensions is a key issue to optimize EUVL source.

This work was supported by Cymer Inc. and by the University of California under the UC Industry-University Cooperative Research Program, award #ele06-10278.

- ¹W. Silfvast and N. Ceglio, *Appl. Opt.* **32**, 6895 (1993).
- ²T. Aota and T. Tomie, *Phys. Rev. Lett.* **94**, 015004 (2005).
- ³S. S. Harilal, M. S. Tillack, Y. Tao, and B. O'Shay, *Opt. Lett.* **31**, 1549 (2006).
- ⁴T. Okuno, S. Fujioka, H. Nishimura, Y. Tao, K. Nagai, Q. Gu, N. Ueda, T. Ando, K. Nishihara, T. Norimatsu, N. Miyanaga, Y. Izawa, K. Mima, A. Sunahara, H. Furukawa, and A. Sasaki, *Appl. Phys. Lett.* **88**, 161501 (2006).
- ⁵C. Koay, S. George, K. Takenoshita, R. Bernath, E. Fujiwara, M. Richardson, and V. Bakshi, *Proc. SPIE* **5751**, 279 (2005).
- ⁶Y. Tao, M. S. Tillack, S. S. Harilal, K. L. Sequoia, and F. Najmabadi, *J. Appl. Phys.* **101**, 023305 (2007).
- ⁷I. Fomenkov, D. Brandt, A. N. Bykanov, A. I. Ershov, W. N. Partlo, D. W. Myers, N. R. Bowering, G. O. Vaschenko, O. V. Khodykin, J. R. Hoffman, E. Vargas, R. D. Simmons, J. A. Chavez, and C. P. Chrobak, *Proc. SPIE* **6517**, 277 (2007).
- ⁸T. Ando, S. Fujioka, H. Nishimura, N. Ueda, Y. Yasuda, K. Nagai, T. Norimatsu, M. Murakami, K. Nishihara, N. Miyanaga, Y. Izawa, K. Mima, and A. Sunahara, *Appl. Phys. Lett.* **89**, 151501 (2006).
- ⁹M. Yamaura, S. Uchida, A. Sunahara, Y. Shimada, H. Nishimura, S. Fujioka, T. Okuno, K. Hashimoto, K. Nagai, T. Norimatsu, K. Nishihara, N. Miyanga, Y. Izawa, and C. Yamanaka, *Appl. Phys. Lett.* **86**, 181107 (2005).
- ¹⁰K. Nagai, Q. Gu, Z. Gu, T. Okuno, S. Fujioka, H. Nishimura, Y. Tao, Y. Yasuda, M. Nakai, T. Norimatsu, Y. Shimada, M. Yamaura, H. Yoshida, M. Nakatsuka, N. Miyanaga, K. Nishihara, and Y. Izawa, *Appl. Phys. Lett.* **88**, 094102 (2006).
- ¹¹Y. Tao, F. Sohbatazadeh, H. Nishimura, R. Matsui, T. Hibino, T. Okuno, S. Fujioka, K. Nagai, T. Norimatsu, K. Nishihara, N. Miyanaga, Y. Izawa, A. Sunahara, and T. Kawamura, *Appl. Phys. Lett.* **85**, 1919 (2004).
- ¹²P. Hayden, J. White, A. Cummings, P. Dunne, M. Lysaght, N. Murphy, P. Sheridan, and G. O'Sullivan, *Microelectron. Eng.* **83**, 699 (2006).
- ¹³L. B. Da Silva, T. W. Barbee, Jr., R. Cauble, P. Celliers, D. Ciarlo, S. Libby, R. A. London, D. Matthews, S. Mrowka, J. C. Moreno, D. Ress, J. E. Trebes, A. S. Wan, and F. Weber, *Phys. Rev. Lett.* **74**, 3991 (1995).
- ¹⁴Y. Tao, S. S. Harilal, M. S. Tillack, K. L. Sequoia, B. O'Shay, and F. Najmabadi, *Opt. Lett.* **31**, 2492 (2006).
- ¹⁵Y. Tao, H. Nishimura, S. Fujioka, A. Sunahara, M. Nakai, T. Okuno, N. Ueda, K. Nishihara, N. Miyanaga, and Y. Izawa, *Appl. Phys. Lett.* **86**, 201501 (2005).